Title
ENERGY LEVELS OF 90Nb POPULATED BY THE DECAY OF 90 Mo

Authors
Cooper, J.A.
Hollander, J.M.
Rasmussen, J.A.

Publication Date
1967-10-01

UCRL-17104

c. 2

University of California

Ernest O. Lawrence Radiation Laboratory

ENERGY LEVELS OF ^{90}Nb POPULATED BY THE DECAY OF ^{90}Mo

J. A. Cooper, J. M. Hollander, and J. O. Rasmussen

October 1967

Berkeley, California

DISCLAIMER

to be submitted to Nucl. Phys.

UCRL-17104
Preprint

UNIVERSITY OF CALIFORNIA

Lawrence Radiation Laboratory
Berkeley, California

AEC Contract No. W-7405-eng-48

ENERGY LEVELS OF ^{90}Nb POPULATED BY THE DECAY OF ^{90}Mo

J. A. Cooper, J. M. Hollander, and J. O. Rasmussen

October 1967

ENERGY LEVELS OF ^{90}Nb POPULATED BY THE DECAY OF ^{90}Mo

J. A. Cooper,† J. M. Hollander, and J. O. Rasmussen

University of California and Lawrence Radiation Laboratory
University of California
Berkeley, California

October 1967

ABSTRACT

The energy levels of ^{90}Nb populated by the decay of 5.7-h ^{90}Mo have been studied with the use of high-resolution germanium γ-ray spectrometers. The γ-ray spectrum revealed a number of low-intensity transitions in addition to the intense 122- and 257-keV lines. The multipolarities of most of these transitions were determined by means of K-shell conversion coefficients, which were calculated from the photon intensities measured in this work together with previously reported conversion electron intensities. In addition, coincidence relationships among the more intense transitions were studied with γ-γ coincidence systems using Ge(Li)-Ge(Li) and Ge(Li)-NaI(Tl) detectors. These and previously reported data have been used to construct a decay scheme in which all of the transitions of greater than 1% intensity are placed. The low-energy transition depopulating the 24-sec isomeric state has not been observed directly, but from lifetime considerations its multipolarity is interpreted as M2, and from energy differences its energy is inferred as 2.38 ±0.36 keV.

---

†Present address: Battelle Memorial Institute, Pacific Northwest Laboratory, Richland, Washington.

1. Introduction

The odd-odd nucleus ^{90}Nb, with 41 protons and 49 neutrons, can be described in terms of the simple shell model as having one "particle" outside the 40-nucleon shell and one "hole" outside the 50-nucleon shell. Thus, it is expected that the lowest-lying levels are composed of the $g_{9/2}$ proton and neutron orbitals, and exhibit spins 9, 8, 7, ..., 0 with even parity. The Brennan-Bernstein rule[1], based on experimental data and δ-force calculations[2], suggests that the ground state of ^{90}Nb has spin 8 and even parity, as do also the tensor-force calculations of Kim and Rasmussen[3]. Experimental information on the decay of ^{90}Nb to ^{90}Zr also supports this assignment[4,5].

The low-lying excitation spectrum of ^{90}Nb is expected to involve, in addition to $P(g_{9/2})N(g_{9/2})^{-1}$ states, also the $p_{1/2}$ orbital, which occurs as the first excited state in the neighboring odd-proton and odd-neutron nuclei. The $g_{9/2},p_{1/2}$ combination produces states of spin and parity 4 and 5, odd. In $^{91}_{41}Nb_{50}$ the $g_{9/2}$-$p_{1/2}$ orbital energy separation is only 100 keV and in $^{89}_{40}Sr_{49}$ it is 600 keV, so it is expected that $P(p_{1/2})N(g_{9/2})^{-1}$ states will be fairly low in the ^{90}Nb excitation spectrum.

The electron-capture and positron decay of 5.7-h $^{90}_{42}$Mo leads to ^{90}Nb excited states, and recently several experimental investigations of this decay have been reported[6-9]. In a study of the γ-ray and internal-conversion electron spectra, Cooper et al.[6]) determined the energies and intensities of 16 γ rays ranging from 43 to 1463 keV. From measurements of the L-subshell conversion intensities the two most prominent transitions, 122 and 257 keV, were found to have multipolarity E2 and E3, respectively. From these data and from considerations of the available shell model states for ^{90}Nb, a partial

decay scheme was proposed that incorporates the 122- and 257-keV transitions but also requires the presence of an undetected low-energy (< 3 keV) isomeric transition in ^{90}Nb. The presence of this low-energy transition was later verified by Cooper et al.[8]), by means of an experiment in which the lifetime of the 24-sec isomeric state was altered by a change of chemical environment. The isomeric transition was not seen directly. The partial level scheme of ^{90}Nb proposed by Cooper et al.[8]) is shown in fig. 1.

More recently Pettersson et al.[9]) have reported the results of a study of the positron and conversion electron spectra of ^{90}Mo. They assigned probable multipolarities to the more intense transitions, as determined from K/L conversion ratios and K-shell conversion coefficients. (The conversion coefficients of Pettersson et al. were calculated from their conversion line intensities and the previously reported photon intensities of Cooper et al.[6]). On the basis of these data plus transition-energy sums and intensities, they proposed a decay scheme for ^{90}Mo that includes all but one of the observed transitions.

The purpose of the work reported here was to reinvestigate the decay scheme of ^{90}Mo with use of improved Ge(Li) γ-ray detectors, in singles and coincidence arrangements. The re-examination of the γ-ray spectrum was undertaken with the object of improving the accuracy of the photon intensities and therefore of the K-shell conversion coefficients. It was also hoped that γ-γ coincidence studies with Ge(Li)-Ge(Li) and Ge(Li)-NaI(Tl) detector systems would define with greater certainty the levels of ^{90}Nb.

2. Experimental Method

The ^{90}Mo activity for the γ-ray spectroscopic studies and for one coincidence experiment was produced by bombarding niobium foils with 50- and 55-MeV protons in the Berkeley 224-cm cyclotron. The ^{90}Mo source for another coincidence experiment was produced by bombarding zirconium foils with 65-MeV α particles.

The chemical procedures used to purify and prepare sources of ^{90}Mo for γ-ray spectroscopy have been described by Cooper et al.[6]). An ion-exchange column in which Mo activity was absorbed served as the source for both the singles and coincidence experiments. To prevent the daughter activity (^{90}Nb) from growing-in, the column was continuously washed with an elutant solution for Nb. To maintain constancy of the counting rate and to make long counting internals possible, ^{90}Mo activity was periodically added to the column.

The γ-ray singles spectrum was studied with a lithium-drifted germanium detector with an active volume of 1 cm^2 by 5 mm deep. The resolution of this detector (FWHM) was 1.3 keV at an energy of 122-keV (^{57}Co). The container of this detector has a 0.010-in. Be window and the detector has a "dead-layer" of about one micron of gold. The associated electronics consisted of the Goulding-Landis "198" biased-amplifier system[10,11]) with a preamplifier containing a cooled field-effect transistor as the first stage[12]). Pulse-height analysis of the spectrum was made with a 1600-channel analyzer.

The γ-ray coincidence spectrum was studied with two germanium detectors (with active volumes 6 cm^2 by 9 mm deep, and 6 cm^2 by 7 mm deep), and a 1-1/2 by 2-in. NaI(Tl) scintillator was also used in some experiments. The containers of the Ge(Li) detectors have 0.020-in. Al windows and the detectors have "dead-layers" of about 1 mm. The "fast-slow" coincidence circuitry was

assembled from units of the "198" system. This equipment uses a "crossover" circuit to generate the fast-coincidence pulses at the crossover points of the slower pulses from the linear amplifiers. A resolving time of 50 nsec was used. Pulse-height analysis of the coincidence spectrum was made with three 400-channel analyzers.

Two coincidence experiments were performed. The first was done with a ^{90}Mo source in which ^{90}Mo and ^{93m}Mo had been produced in about equal amounts by bombarding natural zirconium with 65-MeV α particles. The source for the second experiment was produced by bombarding ^{93}Nb with 50-MeV protons. Very little ^{93m}Mo was produced in the latter bombardment. In both experiments the ion-exchange column containing the activity was placed between the two Ge(Li) detectors (at a source-to-detector distance of about 1 cm), and the angle between the two Ge(Li) detectors was 180 deg.

In the first experiment, the Ge(Li)-Ge(Li) system was used. A single-channel analyzer was used as a "gate" to select a portion of the spectrum, and the detector pulses in coincidence with the gate pulses were displayed on a multichannel analyzer. The smaller detector was used for gating on several of the lower-energy γ rays, and the coincident γ-ray spectrum was detected with the larger detector. In the second experiment, a NaI(Tl) detector was used to gate on high-energy γ rays while the small Ge(Li) detector was used to gate on low-energy γ rays, and the γ-ray spectra in coincidence with the two gates were recorded simultaneously. Because of the large number of 180-deg Compton scattered γ rays detected by the Ge(Li) detectors with the geometry used, it was necessary to record spectra in coincidence with the Compton backgrounds on both sides of the photopeaks as well as spectra in coincidence with the photopeaks themselves.

3. Experimental Results

3.1 GAMMA-RAY SPECTRUM

In the initial study of ^{90}Mo by Cooper et al.[6]), 16 photon lines were observed. The existence of these was verified in the study of the internal conversion spectrum by Pettersson et al.[9]), who found in addition a transition at 1482 keV. In the present study, 23 γ-ray lines have been identified in the Ge(Li) spectrum as arising from the decay of ^{90}Mo. The assignment of these lines to ^{90}Mo rather than to ^{93m}Mo, to the daughter ^{90}Nb, or to other isotopes, was based on several considerations including that of the high chemical purity of the ^{90}Mo sources and also of the fact that these lines were not observed in spectra of pure ^{93m}Mo or ^{90}Nb.

A sample ^{90}Mo gamma spectrum is reproduced in figs. 2 and 3, and the energy and intensity data are summarized in Table 1, together with other information. The relative photon intensities were computed with use of a photopeak efficiency function experimentally determined for this detector by Haverfield[13]). Several observations can be made concerning the gamma-ray spectrum:

a. One notes in the figures several peaks marked as "double-escape" peaks arising from high-energy γ rays of ^{90}Mo, ^{90}Nb, or ^{93m}Mo. Some of the intensity of the 365 and 455 peaks is probably due to γ rays of these energies, as the double-escape-peak to photopeak ratios are abnormally high in these cases.

b. The indium x rays (fig. 2) arise from γ-ray interactions with the indium metal used to make electrical contact with the detector. The lead x rays were produced in nearby shielding blocks.

Table 1

Summary of ^{90}Mo transition energies, intensities, and internal conversion coefficients

Transition[a] energy (keV)	Photon[b] intensity (percent)	Conversion shell	Conversion[b,c] electron intensity (percent)	Transition[b] intensity (percent)	Internal Conversion Coefficient (experimental)	(theoretical) M1	(theoretical) E2
42.70 ± 0.04	2.18 ± 0.2	K	4.8 ± 1.6	7.5 ± 1.7	2.2 ± 0.7 (0)	2.4 (0)	---
		L	0.50 ± 0.13		2.3 ± 0.6 (-1)	2.9 (-1)	8.1 (0)
122.370 ± 0.022	65.34 ± 2.4	K	28.86 ± 0.7	100	4.4 ± 0.4 (-1)	1.2 (-1)	4.6 (-1)
		L	4.79 ± 0.10		7.3 ± 0.9 (-2)	1.5 (-2)	7.7 (-2)
		M+N	1.04 ± 0.13				
162.93 ± 0.09	6.06 ± 0.5	K	0.342 ± 0.013	6.45 ± 0.5	5.6 ± 0.8 (-2)	5.5 (-2)	1.7 (-1)
		L	0.038 ± 0.003		6.3 ± 1.4 (-3)	6.5 (-3)	2.5 (-2)
		M+N	0.009 ± 0.003				
203.13 ± 0.10	6.46 ± 0.5	K	0.209 ± 0.006	6.70 ± 0.5	3.2 ± 0.6 (-2)	3.1 (-2)	7.9 (-2)
		L	0.026 ± 0.002		4.0 ± 1.0 (-3)	3.6 (-3)	1.1 (-2)
		M+N	0.006 ± 0.004				
257.34 ± 0.04	79.1 ± 2.6	K	11.23 ± 0.4	92.8 ± 2.7	1.42 (-1)		E3 1.42 (-1)
		L	2.04 ± 0.06		2.6 ± 0.4 (-2)		2.6 (-2)
		M+N	0.40 ± 0.03		5.1 ± 1.0 (-3)		---
323.20 ± 0.18	6.41 ± 0.5	K	0.0642 ± 0.0020	6.48 ± 0.5	1.0 ± 0.1 (-2)	0.9 (-2)	1.5 (-2)
		L	0.0074 ± 0.0006		1.2 ± 0.3 (-3)	1.1 (-3)	
421.0 ± 0.3	0.25 ± 0.08	K	0.00092 ± 0.00014	0.25 ± 0.08	3.6 ± 0.7 (-3)	4.9 (-3)	6.7 (-3)
425.1 ± 0.5*	0.36 ± 0.08		---	0.36 ± 0.08			
440.5 ± 0.6*	0.95 ± 0.2		---	0.95 ± 0.2			
445.37 ± 0.21	6.13 ± 0.6	K	0.0288 ± 0.0018	6.16 ± 0.6	4.7 ± 0.9 (-3)	4.2 (-3)	5.6 (-3)
		L	0.0025 ± 0.0011				
472.24 ± 0.28	1.45 ± 0.15	K	0.0040 ± 0.0002	1.45 ± 0.15	2.8 ± 0.7 (-3)	3.7 (-3)	4.7 (-3)
489.8 ± 0.4	0.74 ± 0.1	K	0.0027 ± 0.0003	0.74 ± 0.1	3.7 ± 1.0 (-3)	3.5 (-3)	4.2 (-3)
517.7 ± 0.7*	0.16 ± 0.1		---	0.16 ± 0.1			
941.5 ± 0.4	5.62 ± 0.6	K	0.00377 ± 0.00013	5.62 ± 0.6	6.7 ± 1.2 (-4)	7.6 (-4)	7.4 (-4)
946.4 ± 0.8*	0.68 ± 0.2		---	0.68 ± 0.2			
987.3 ± 1*	0.14 ± 0.05		---	0.14 ± 0.05			
990.2 ± 0.6	1.04 ± 0.1	K	0.00069 ± 0.00008	1.04 ± 0.1	6.6 ± 1.7 (-4)	6.8 (-4)	6.6 (-4)
1271.3 ± 0.6	4.17 ± 0.4	K	0.00196 ± 0.00014	4.17 ± 0.4	4.7 ± 1.0 (-4)	5.1 (-4)	4.9 (-4)
1387.4 ± 0.5	1.88 ± 0.2	K	0.00079 ± 0.00005	1.88 ± 0.2	4.2 ± 0.9 (-4)	5.4 (-4)	3.2 (-4)
1446 ± 2*	0.05 ± 0.02			0.05 ± 0.02			
1454.6 ± 0.7	1.91 ± 0.5	K	0.00064 ± 0.00007	1.91 ± 0.5	3.3 ± 1.6 (-4)	2.0 (-4)	1.9 (-4)
1463.5 ± 0.9	0.68 ± 0.2	K	0.00031 ± 0.00010	0.68 ± 0.2	4.5 ± 3.6 (-4)	2.0 (-4)	1.9 (-4)
1481.6 ± 1.4	0.21 ± 0.2	K	0.00032 ± 0.00016	0.21 ± 0.2			

[a] All quoted transition energies except those marked *, are the values determined by Pettersson et al.[9]).

[b] The quoted intensities are absolute values in percent of total ^{90}Mo decays, normalized to 100% intensity for the 122 keV transition.

[c] Conversion line relative intensity values were taken from Pettersson et al.[9]), and these were normalized to the photon relative intensities by use of the value 0.142 for the K-conversion coefficient of the 257-keV E3 transition.

c. It was possible to obtain a more accurate relative intensity value of the 42.7-keV photon than in our previous work[6] because of the much lower absorption of low-energy γ rays by the very thin "dead-layer" and window of the new detector used in this study.

d. Special mention should be made of the 425.1-keV γ ray seen in our γ-ray spectrum of ^{90}Mo. Pettersson et al.[9] report observing a conversion line that they assign to a 423.4-keV transition in the daughter ^{90}Nb, on the basis of half-life information. We have however examined the γ-ray spectrum of pure ^{90}Nb sources, and no γ rays were found in the vicinity of 423 keV (see fig. 34, ref. 14). If we reassign the conversion line observed by Pettersson et al. to the decay of ^{90}Mo, the transition energy becomes 424.4 ±0.3 keV, which is consistent with our value 425.1 ±0.5 keV.

3.2 COINCIDENCE STUDIES AND LEVEL ENERGIES

a. Levels at 854, 2126, and 2309 keV

The ^{90}Nb level scheme proposed by Pettersson et al.[9] differs in essential respects from the one that evolved from our studies (fig. 4) and these differences are best described with reference to the coincidence data on which our level scheme is based.

A major feature of the level scheme resulting from the coincidence information is that the 43, 163, 203, and 323-keV transitions are <u>in cascade</u>, with no strong crossover transitions. This contradicts the scheme of Pettersson et al., which shows the 43-323 pair occuring <u>in parallel</u> with the 163-203 pair. The data bearing on this point are shown in figs. 5 through 8. Evidence for

the simple cascade relationship comes from the fact that the relative intensities of the 43, 163, 203, and 323-keV photopeaks are equal, in the three coincidence spectra taken by gating with the 163, 203, and 323 γ lines, as well as in the singles spectrum (Table 2). The same is true of the 1271 and 1455 photopeaks, and we conclude that the latter two transitions feed the cascade. (See section d below for further discussion of 1455-keV coincidences.) The data also show that the 490- and 990-keV transitions are in coincidence with the 163-keV transition.

It is interesting to take note of the sum relationship $E_{43\gamma} + E_{323\gamma} = E_{163\gamma} + E_{203\gamma}$ which was the basis for the conclusion by Pettersson et al. that these two pairs of transitions de-excite a common level in parallel. Because of the coincidence results, however, we conclude that this sum is accidental.

In constructing the level scheme, it is necessary to establish first the base state of the 163- cascade. (In the following, "the 163- cascade" refers to the 43, 163, 203, 323 series of γ rays, with sequence unspecified.) The possible choices, from the basic level scheme of fig. 1, are the ground state, either of the isomeric states (1+ or 4-), or the 6+ state at 122.4 keV. We rule out the 1+ state on the basis that ^{90}Mo has insufficient decay energy available to allow the 163- cascade plus 1455-keV transition to feed this state. The choice of decay to ground can be eliminated on angular momentum arguments; that is, the maximum spin change that can be brought about by the electron capture plus the γ-ray cascade (starting with the 1271-keV transition) is 7 units, according to multipolarity and log ft information discussed in Section 4, whereas the spin difference between parent and daughter ground states is 8 units. Of the remaining states, 4- or 6+, the even parity state is chosen because of the magnetic dipole character of the transitions in the

Table 2

Relative intensities[a] of the 43-, 163-, 203- and 323-keV gamma rays in the coincidence spectra

Gate energy (keV)	A/B	C/B	D/B
163[b,c]	0.25 ± 0.03	0.64 ± 0.04	0.26
203[b]	0.29 ± 0.03		0.26 ± 0.02
323[b]	0.22 ± 0.04	0.64 ± 0.07	
163[d,e]	0.265	0.68 ± 0.02	0.26 ± 0.02
942[d]	0.24 ± 0.03	0.68 ± 0.03	0.25 ± 0.03
1130[d]	0.29 ± 0.03	0.68 ± 0.03	0.27 ± 0.03
1387[d]	0.26 ± 0.05	0.72 ± 0.03	0.26 ± 0.03
Singles		0.68 ± 0.05	0.26 ± 0.02

A = intensity of the 43-keV photopeak

B = intensity of the 163-keV photopeak

C = intensity of the 203-keV photopeak

D = intensity of the 323-keV photopeak

[a]The intensities have not been corrected for photopeak efficiencies.

[b]Obtained from first experiment, Zr (α, xn) Mo^{90}.

[c]These relative intensities were normalized to the 323-keV photopeak intensity.

[d]Obtained from second experiment, Nb^{93} (p, 4n) Mo^{90}.

[e]These relative intensities were normalized to the 43-keV photopeak intensity.

cascade and those feeding it, and because the high-lying states receiving the primary electron-capture decay appear to have even parity. (The fact that the 122-keV transition, de-exciting the 6+ state, was not observed in coincidence with any members of the 163-cascade might be regarded as evidence against this interpretation, but it is likely that the half-life of this state is much longer than the 50-nsec resolving time used in the coincidence experiments.)

We note that the foregoing arguments, which define levels at 854.3, 2125.6, and 2308.9 keV, do not establish the sequence of the 43-, 163-, 203-, and 323-keV transitions in the cascade.

b. Levels at 1844 and 2334 keV

The following energy sum of the type $E_1 + E_2 = E_3$ is valid within the experimental errors, and indicates a cascade-crossover relationship: $E_{990\gamma} + E_{490\gamma} = E_{1482\gamma}$. The coincidence data indicate that both the 490- and 990-keV transitions are in coincidence with the 163- cascade. The 990 is the more intense so we place it below the 490. Thus, levels are located at 1844.5 and 2334.3 keV. In support of this interpretation one notes that the ratio of the relative intensity of the 990-keV peak in the coincidence spectrum to that in the singles spectrum is 0.90 ±0.13 while that calculated from our proposed decay scheme (fig. 4) is 0.83 ±0.04. The same quantities for the 490-keV transition are 0.56 ±0.05 and 0.48 ±0.1, respectively.

c. Placement of the 472-keV transition; energy of the 24-sec isomeric transition.

The position of the 472-keV transition in the decay scheme is, in our interpretation, the key to the determination of the energy of the 24-sec ^{90}Nb isomer. A cascade-crossover relation is indicated by the energy sum, $E_{472\gamma} + E_{990\gamma} = E_{1463\gamma}$, which is satisfied within experimental error. The

472-keV transition cannot precede the 990, as does the 490, because in that case there could be no incoming-outgoing intensity balance at the 1844-keV level. Therefore, the 472 is placed below the 990 and a level is defined at 382.1 keV. The coincidence data strongly support this interpretation; in addition to the fact, already mentioned, that the 990-keV γ ray was observed in coincidence with the 163- cascade, the data also revealed that the 472-keV γ ray definitely was not in coincidence with the 163- cascade. This confirms that the 472-keV transition does not precede the 990-keV transition. (In the scheme given by Pettersson et al., both the 472- and 490-keV transitions precede the 990-keV transition, but this situation contradicts both the coincidence and intensity arguments presented here.)

The energy of the isomeric transition is calculated by closing the energy cycle shown in fig. 9. The validity of this cycle is supported by the good incoming-outgoing intensity balance at the 122.4-keV state. Thus the value of E_{IT}, determined in this way, is 2.38 ±0.36 keV. Note that this value and its error are independent of the relative order of the transitions in the 163- cascade since only the sum of the transition energies in the cascade enters the calculation.

This result is consistent with the 3-keV upper limit placed on the transition energy by our previous study[6]. Intense electron lines, observed below 2.5 keV in the earlier study but unidentified because of insufficient resolution, would be consistent with the expected predominant M_I and M_{III} conversion lines of a 2.38-keV M2 transition, which would occur at 1.91 and 2.01 keV.

d. The level at 1769 keV

The existence of a level at 1769 keV is indicated by energy-sum, intensity, and coincidence data. Good agreement in the energy sums $E_{445\gamma} + E_{942\gamma} = E_{1387\gamma}$

and $E_{441\gamma} + E_{946\gamma} = E_{1387\gamma}$ suggests a cascade-crossover relation, and this is substantiated by the coincidence spectrum shown in fig. 10. The only high-energy γ ray definitely in coincidence with the 445-keV γ ray (gate) was the 942-keV γ ray. No low-energy coincidences were observed.

For verification, it was desirable to examine the spectra in coincidence with the 942- and 1387-keV γ rays, but the poor resolution of the NaI detector made it impossible to select individual photopeak "gates" in the high-energy region. Thus, the gate "window" set over the 942-keV photopeak also included the 946-, 987-, and 990-keV photopeaks. The γ-ray spectrum in coincidence with this gate, shown in fig. 11, clearly shows the 445-keV γ ray and confirms the 445-942 coincidence relation. (One also sees 163, 203, 323 coincidences because of the 990-keV component of the gate window.)

The spectrum in coincidence with the 1387-keV gate, which includes the 1387-, 1446-, 1455-, 1463-, and 1481-keV γ rays (fig. 12), shows all four members of the 163 cascade with the same relative intensity that they have in the singles spectrum. We interpret this as being due primarily to the 1455-keV component of the gate pulses. It is reasoned that essentially none of these coincidences can be due to the 1387-keV gamma ray because this line did not appear in the spectrum in coincidence with the 163-keV gate (fig 6). If the 1387 were in coincidence with any of the other members of the cascade (43-, 203-, 323-), the intensity of the 163-keV photopeak in fig. 12 would have been noticeably low. It is also known from the 163-keV coincidence spectrum that the 1455-keV γ ray is in coincidence with the 163-keV γ ray. Thus, if the 1455-keV transition were not in coincidence with all 4 of these low-energy γ rays, one, two, or three of them would have had an intensity noticeably lower than the 163-keV photopeak intensity.

The placement of the 445-942 cascade in the level scheme was made on the basis of the following arguments:

1. Since no prominent transitions were found to be in coincidence with the 445-, 942-, or 1387-keV γ rays, the intensity of this cascade (~8% of total decays of ^{90}Mo) must be due to primary electron-capture decay to the 1769-keV level.
2. The lack of coincidences also indicates that the 445-942 cascade feeds a state with lifetime much greater than the resolving time, 50 nsec. The 4- (124.8 keV), and the 1+ (382.1 keV) are such states, and the 6+ (122.4 keV) is probably such a state. Of these states, the 6+ and 4- are already associated with ~100% feeding intensity. (The sum of the 257-keV transition intensity and that of the 163-keV cascade is actually about 99.2%.) Since the intensity of the 445-942 cascade is about 8%, it cannot possibly bypass the 257-keV transition.

Thus, the data indicate that the 445-942 keV and 441-946 keV cascades feed the 1+ state at 382.1 keV and therefore a state at 1769.0 is defined. The order of the transitions in these cascades is not certain, since their intensities are about equal. However, we take note of an energy sum of the type $E_1 + E_2 = E_3 + E_4$ which, if not accidental, would indicate that the 942-keV transition lies lower than the 445-keV transition. The sum is:

$E_{942\gamma} + E_{987\gamma} = E_{472\gamma} + E_{1455\gamma}$.

3.3 TRANSITION INTENSITIES, CONVERSION COEFFICIENTS, AND MULTIPOLARITY ASSIGNMENTS

In Table 1 a summary is given of all the energy, intensity, and multipolarity data on the ^{90}Mo transitions. In constructing this table, the photon intensity data obtained in this work were combined with the conversion electron data of Pettersson et al.[9]), to give relative values of the internal conversion coefficients. From these, absolute values were computed by normalizing to the Sliv and Band theoretical value[15]) for the 257-keV E3 transition. In the table, all photon and electron intensities are given as percentages of ^{90}Mo decay; the normalizing factor used here was obtained from our knowledge of the absolute intensity of the 122-keV transition (100%).

For a comparison of the experimental conversion coefficients of all transitions (except the 2.4- and 42.7-keV transitions) with the theoretical values, fig. 13 was prepared. From this plot a definite multipolarity assignment of M1 is made to the 163-, 203-, and 323-keV transitions. All others appear to be M1, E2 or mixed M1-E2 transitions.

In our previous investigation[6]), the L-subshell electron lines of the 42.7-keV transition were recorded with the Berkeley 50-cm iron-free spectrometer. The experimental $L_I/(L_{II} + L_{III})$ ratio for this transition is 10.5 ±1.5. The theoretical ratios (determined from log-log plots of values in the Sliv and Band tables) for E1, E2, M1, and M2 multipolarities are 3.28, 0.220, 10.9, and 7.6, respectively. Thus, it appears that the 42.7-keV transition is also predominantly M1.

3.4 THE 2.4-keV ISOMERIC TRANSITION

Of central importance to our understanding of the ^{90}Nb level scheme is the multipolarity of the 2.4-keV isomeric transition, since the considerations of angular momentum and parity conservation that led Cooper et al.[6]) to postulate its existence also restricted the choice of multipolarities to M2 or E3.

One obvious problem in this connection is the lack of direct experimental information on the conversion lines of this transition. We do however know the half-life of the isomeric state, and it would be instructive to compare the reduced photon half-life with theory for different multipolarities. For very low-energy transitions (where the conversion coefficient $\alpha \gg 1$) the reduced photon lifetime is given by

$$\mathcal{T}_{M2} \approx \alpha\tau E_\gamma^5 A^{2/3}$$

$$\mathcal{T}_{E3} \approx \alpha\tau E_\gamma^7 A^2$$

where α = total conversion coefficient

τ = total half-life.

At the time this work was done, there were available no tables of theoretical conversion coefficients for very low-energy transitions converting in outer shells, and it was necessary to make use of extrapolations and approximations in order to estimate them[14]). Recently, however, Hager and Seltzer[16]) have made an extensive calculation of relativistic, screened conversion coefficients including the M-shells, and these calculations have been carried to very low energies so that no extrapolations are necessary for our analysis. In computing the values for the ^{90}Nb isomeric transition, we have estimated the N-subshell coefficients as

one-third the corresponding M-subshell values, and the N_{IV}- and N_V- subshell values were further reduced by the factor 0.4 to correct for the incomplete 4d orbit of niobium. The O_I- subshell value was assumed to be one-sixth the N_I value because the 5s orbit is only half full.

With use of conversion coefficients estimated in this way for the 2.4-keV transition in ^{90}Nb, we have calculated the reduced lifetime values for the M2 and E3 alternatives, and they are plotted in fig. 14 (vs. neutron number). The similarly calculated value for the 2.1 keV isomeric transition in ^{99}Tc, known to be an E3, is also plotted. For reference to known M2 and E3 transitions, we have included also reduced lifetime values taken from the book of Sliv[17]) for these multipoles. This comparison indicates that the ^{90}Nb isomeric transition is a slow M2, which is common, rather than a very fast E3, which is uncommon. Were this transition an E3, its reduced lifetime would in fact be the shortest of any of the known E3 transitions shown in fig. 14. It is interesting to note, however, that the value for the 2.1-keV E3 isomer of ^{99}Tc is considerably shorter than most other E3 transitions.

4. Electron Capture and Positron Decay of ^{90}Mo

4.1 LOG Ft VALUES

The level scheme shown in fig. 4 incorporates 19 out of 23 transitions identified in ^{90}Mo decay, and accounts for 99% of the decay intensity.

The transition intensity data indicate that 82 ±5% of the primary ^{90}Mo decay populates the 1+ state at 382.1 keV. With use of the theoretical EC/β^+ ratio 2.2 ±0.1 (obtained from curves given by Wapstra[18]) and Feenberg and Trigg[19])) we calculate a positron branching to this level of 26 ±1.4%, which

agrees closely with the value 25.5% measured from the positron spectrum by Pettersson et al.[9] Also in agreement is the value for the EC/β^+ branching, 3.0 ±0.5, reported earlier by us[6].

4.2 SPIN AND PARITY ASSIGNMENTS

Our experimental log ft values for EC and β^+ decay, given in fig. 4, indicate that all observed transitions, with the possible exception of that to the 1844-keV state, are of the allowed type. We conclude that the high-lying states shown in the figure have even parity and spin values 0 or 1.

The most prominent new feature of the ^{90}Nb level scheme resulting from this study is the cascade of M1 transitions leading from the 854-keV state to the 6+ state at 122 keV. This cascade seems clearly to be identified with the band of even-parity states expected from the $P(g_{9/2})\ N(g_{9/2})^{-1}$ configuration, and thus we have made the assignment 2+, 3+, 4+, 5+, 6+ for this sequence of levels. As stated before, we have no data bearing on the order of the transitions in the cascade.

5. Theoretical Considerations

The decay scheme and transition energies and intensities obtained for the ^{90}Mo to ^{90}Nb decay should provide valuable tests of nuclear theory. The neighboring nucleus $^{90}_{40}Zr_{50}$ has a closed major neutron shell and a closed proton subshell. Thus, to a first approximation we expect to find in ^{90}Nb the simple multiplet 0+, 1+, ... 8+, 9+ resulting from the interaction of a $g_{9/2}$ proton with a $g_{9/2}$ neutron hole. Figure 15 is taken from the 1963 work of Kim and Rasmussen[20] and shows the expected particle-hole spectrum for $P(g_{9/2})N(g_{9/2})$

in A ~ 90. Their calculation used the "Potential II", including tensor components, that they employed in fitting the spectrum of ^{210}Bi [21]. It is seen that the theoretical spectrum of fig. 15 correctly predicts a cascade 2+, 3+, 4+, 5+, 6+, 8+. The 2+ level lies theoretically ~0.8 MeV above the lowest lying 8+, in surprisingly good agreement with the 854.3 keV of experiment. The smallest energy spacing in the above cascade is expected to be the 4+ to 5+ transition, lending some argument for placement of the 42.7-keV transition in that position.

The theory predicts that the 0+ and 1+ states of the multiplet lie near 2 MeV. The simplest shell model considerations, ignoring residual interactions such as pairing force, would predict that these 0+ and 1+ states should incorporate the predominant beta decay strength and exhibit low log ft values. The parent ^{90}Mo would be assigned predominantly the configuration of a pair of $g_{9/2}$ protons and a pair of $g_{9/2}$ neutron holes outside the ^{90}Zr core. In allowed beta decay a $g_{9/2}$ proton could transform into a $g_{9/2}$ or $g_{7/2}$ neutron, but the latter strength ($g_{7/2}$) would be centered at such high excitation energy in ^{90}Nb that it would be negligible.

Experimentally, we see that the three largest beta decay matrix elements (log ft between 4.5 and 4.7) go to states at 2126, 2309, and 2334 keV. This feature is consistent with the above theoretical considerations if we realize that above ~1 MeV the ^{90}Nb states may have a complex structure with considerable configuration mixing. The beta decay strength may be spread across many states, with the beta decay matrix elements being a measure of the admixture of the simple $[P(g_{9/2})N(g_{9/2})^{-1}]_{0,1+}$ in the various states. The ^{90}Nb states of low spin above 1 MeV may involve core excitation (^{90}Zr has a 0+ excited state at

1.75 MeV and a 2+ at 2.182 MeV) and also configuration mixtures of $[P(p_{1/2})^{-1}(g_{9/2})^2\ N(p_{1/2})^{-1}]_{0,1+}$. The 1+ state at 382.1 keV may be predominantly of the p-state character above. It remains for a more sophisticated shell-model theoretical calculation to make quantitative comparison with experimental energies and transition intensities.

6. Acknowledgements

We are grateful to Professor Gordon Struble for making a preliminary theoretical calculation of the spectrum of ^{90}Nb using realistic neutron proton forces in a quasi-particle representation. His calculation was important in stimulating the intensive examination of our coincidence data that led to the decay scheme here presented.

We also acknowledge with thanks the assistance rendered by Mr. Fred Bernthal, Mr. Don Davies, Dr. Judd Haverfied, Mr. Martin Holtz, and Professor Stanley Prussin.

This work was supported by the U. S. Atomic Energy Commission.

REFERENCES

1. M. H. Brennan and A. M. Bernstein, Phys. Rev. 120 (1960) 927
2. C. Schwartz, Phys. Rev. 94 (1954) 95
3. J. O. Rasmussen and Y. E. Kim, Izv. Akad. Nauk. 29 (1965) 94
4. N. H. Lazar, G. D. O'Kelley, J. H. Hamilton, L. M. Langer, and W. G. Smith, Phys. Rev. 110 (1958) 513
5. S. Björnholm, O. B. Nielsen, and R. K. Sheline, Phys. Rev. 115 (1959) 1613
6. J. A. Cooper, J. M. Hollander, M. I. Kalkstein, and J. O. Rasmussen, Nucl. Phys. 72 (1965) 113
7. E. P. Grigorev, Yu. S. Egorov, A. V. Zolotavian, V. O. Sergeev, and M. I. Sovtsov, Izv. Akad. Nauk. SSSR, ser. fiz. 29 (1965) 721 (trans.: Acad. Sci. Bulletin Phys. Series 29 (1965) 724)
8. J. A. Cooper, J. M. Hollander, and J. O. Rasmussen, Phys. Rev. Letters 15 (1965) 680
9. H. Pettersson, G. Bäckström, and C. Bergman, Nucl. Phys. 83 (1966) 33
10. F. S. Goulding and D. A. Landis, Techniques in Nuclear Pulse Analysis, National Academy of Sciences, National Research Council, Washington, 1963, Publication 1184
11. F. S. Goulding, Lawrence Radiation Laboratory Report UCRL-11302, Feb. 1964
12. E. Elad and M. Nakamura, Lawrence Radiation Laboratory Report UCRL-16760, 1966
13. A. J. Haverfield, Ph.D. Thesis, Lawrence Radiation Laboratory Report UCRL-16969
14. J. A. Cooper, Ph.D. Thesis, Lawrence Radiation Laboratory Report UCRL-16910
15. L. A. Sliv and I. M. Band, in Alpha-Beta- and Gamma-Ray Spectroscopy, Vol. II ed. by K. Siegbahn, North-Holland Publ. Co., Amsterdam, 1965, p. 1639

16. R. S. Hager and E. C. Seltzer, Calif. Inst. of Technology Report CALT-63-60, June 1967

17. L. A. Sliv, Gamma-Rays, Acad. Sci. USSR, Moscow-Leningrad, 1961

18. A. H. Wapstra, G. J. Nijgh, and R. Van Lieshout, Nuclear Spectroscopy Tables, North-Holland Publishing Co., Amsterdam, 1959

19. E. Feenberg and G. Trigg, Rev. Mod. Phys. 22 (1950) 399

20. J. O. Rasmussen and Y. E. Kim, 1963 Chem. Div. Annual Report, UCRL-11213, p. 25

21. Y. E. Kim and J. O. Rasmussen, Nucl. Phys. 47 (1963) 184

FIGURE CAPTIONS

1. Partial decay scheme of ^{90}Mo proposed by Cooper et al.[8]).
2. Low-energy portion of the gamma-ray spectrum of ^{90}Mo observed with 1 cm^2 × 5 mm deep Ge(Li) detector with cooled F.E.T. preamplifier.
3. High-energy portion of gamma-ray spectrum of ^{90}Mo (with Pb absorber) observed with 1 cm^2 × 5 mm deep Ge(Li) detector with cooled F.E.T. preamplifier.
4. Decay scheme of 5.7 hour ^{90}Mo.
5. Low-energy portion of the gamma-ray spectrum in coincidence with the (A) 163-keV photopeak and (B) Compton background on the high-energy side of the 163-keV photopeak. Also shown for comparison is the singles spectrum.
6. High-energy portion of the gamma-ray spectrum in coincidence with the (A) 163-keV photopeak and (B) Compton background on the high-energy side of the 163-keV photopeak. Also shown for comparison is the singles spectrum.
7. Low-energy portion of the gamma-ray spectrum in coincidence with the (A) Compton background on the low-energy side of the 203-keV photopeak, (B) 203-keV photopeak and (C) Compton background on the high-energy side of the 203-keV photopeak. Also shown for comparison is the singles spectrum.
8. Low-energy portion of the gamma-ray spectrum in coincidence with the (A) Compton background on the low-energy side of the 323-keV photopeak and (B) 323-keV photopeak. Also shown for comparison is the singles spectrum.

9. Energy cycle used to calculate energy of the 24-sec ^{90}Nb isomer.
10. High-energy portion of the gamma-ray spectrum in coincidence with the (A) 445-keV photopeak (B) Compton background on the high-energy side of the 445-keV photopeak.
11. Low-energy portion of the gamma-ray spectrum in coincidence with the (A) "942-keV photopeak" and (B) Compton background on the high-energy side of the "942-keV photopeak".
12. Gamma-ray spectrum in coincidence with the (A) "1387 (+)-keV photopeak" and (B) Compton background on the high-energy side of the "1387 (+)-keV photopeak".
13. Theoretical K-shell internal conversion coefficients plotted against gamma-ray energy. The experimentally determined K-shell coefficients are also shown (points with error bars).
14. Reduced lifetimes of (A) M2 and (B) E3 transitions plotted versus neutron number.
15. Theoretical particle-hole spectrum for A ~ 90, from Kim and Rasmussen [20].

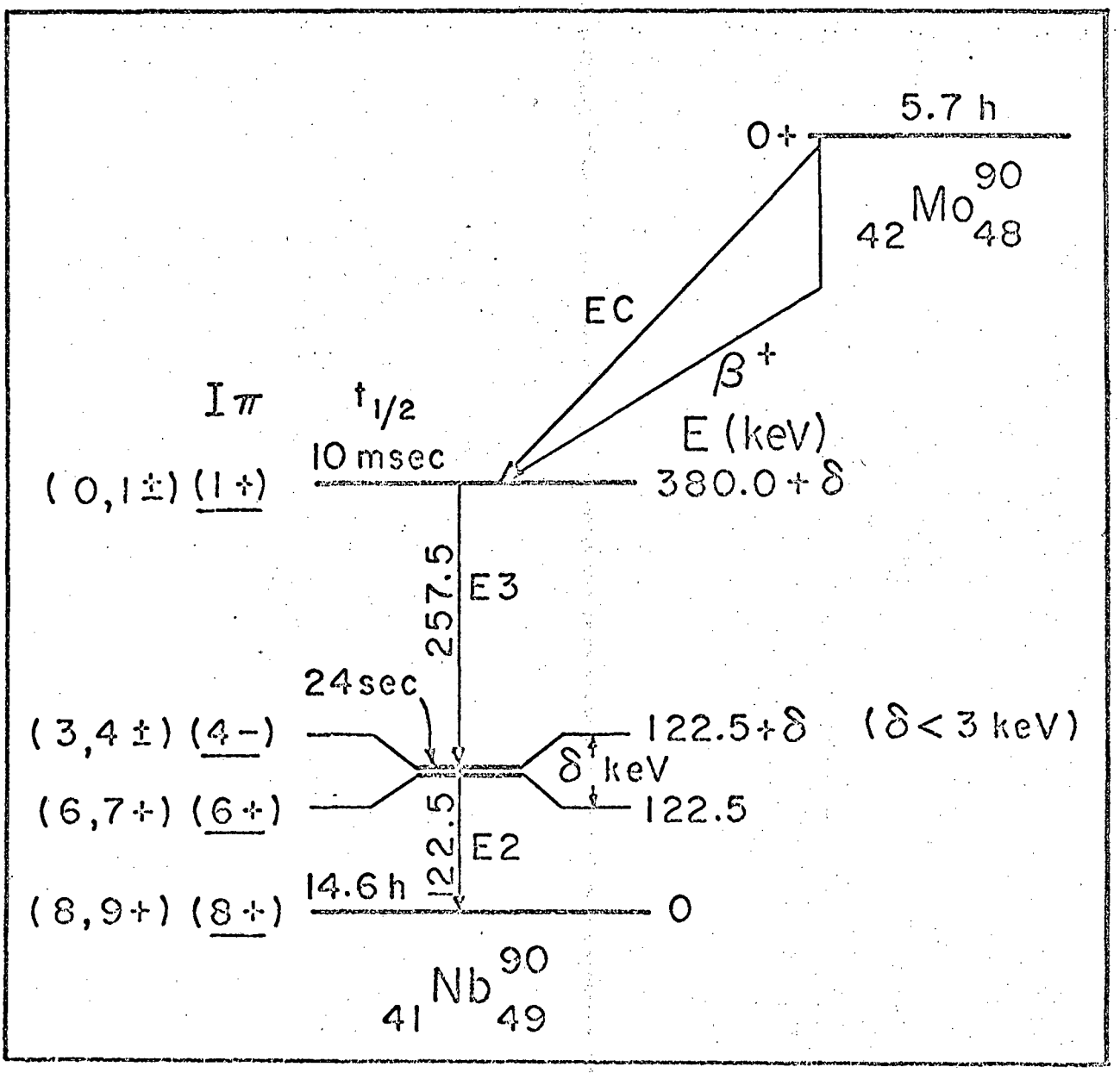

MUB-5035

Fig. 1

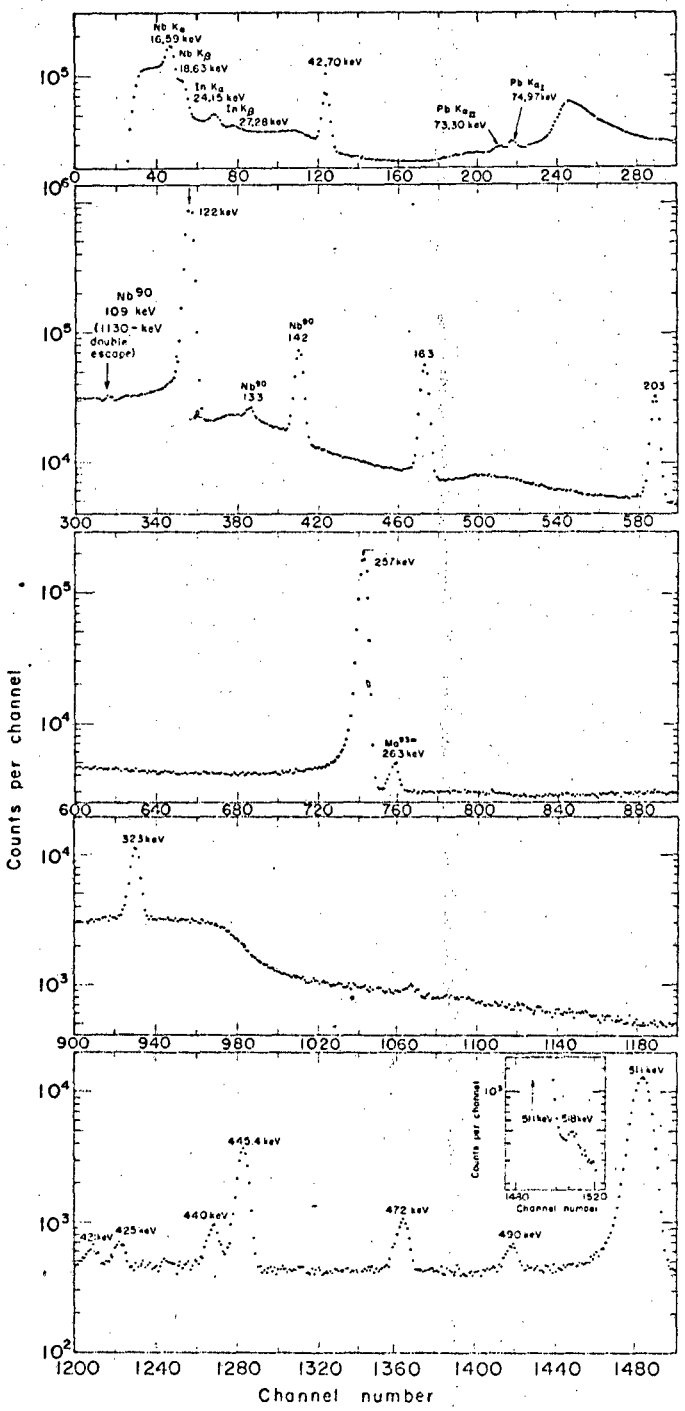

MUB-12579-A

Fig. 2

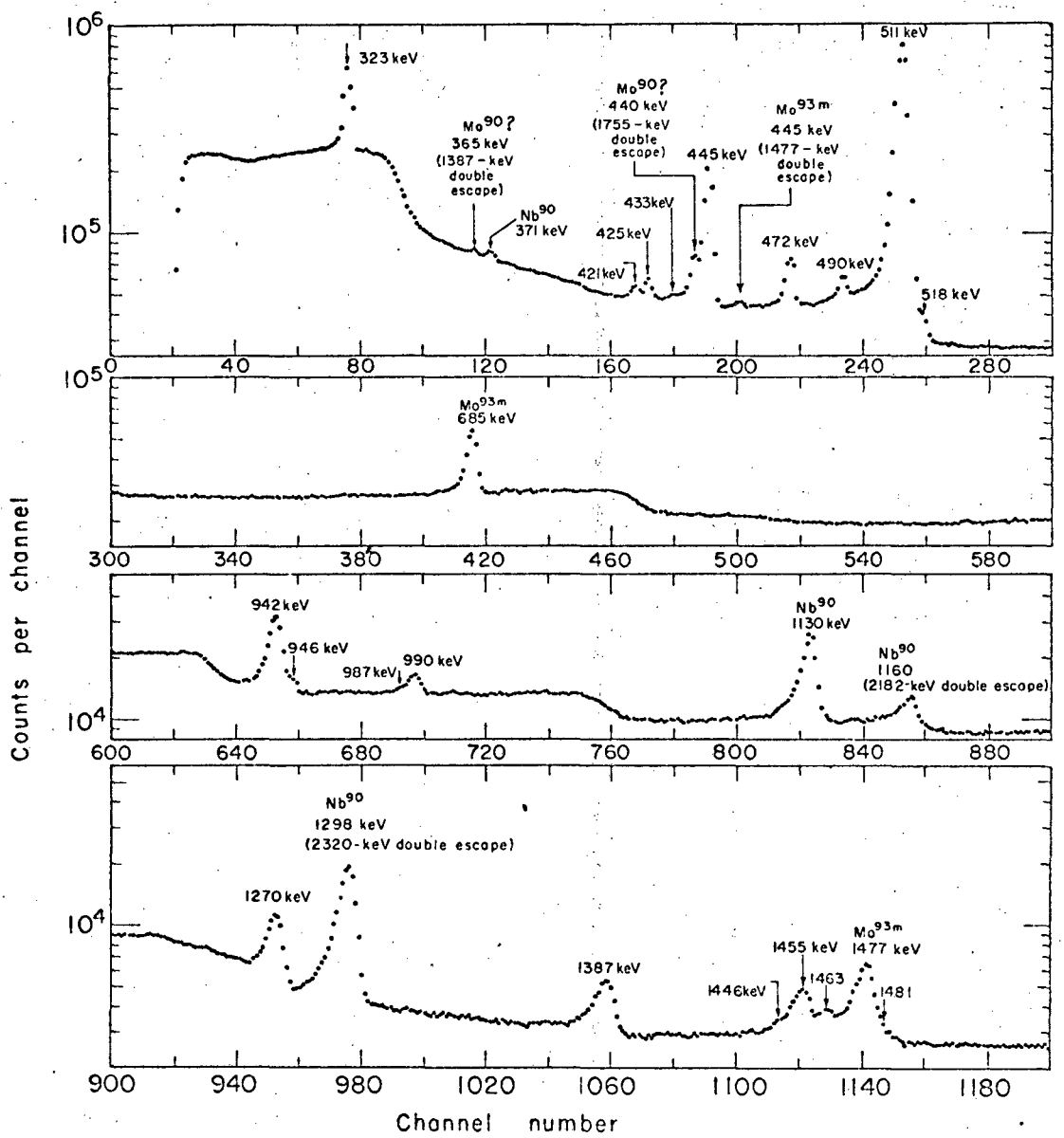

MUB-12572-A

Fig. 3

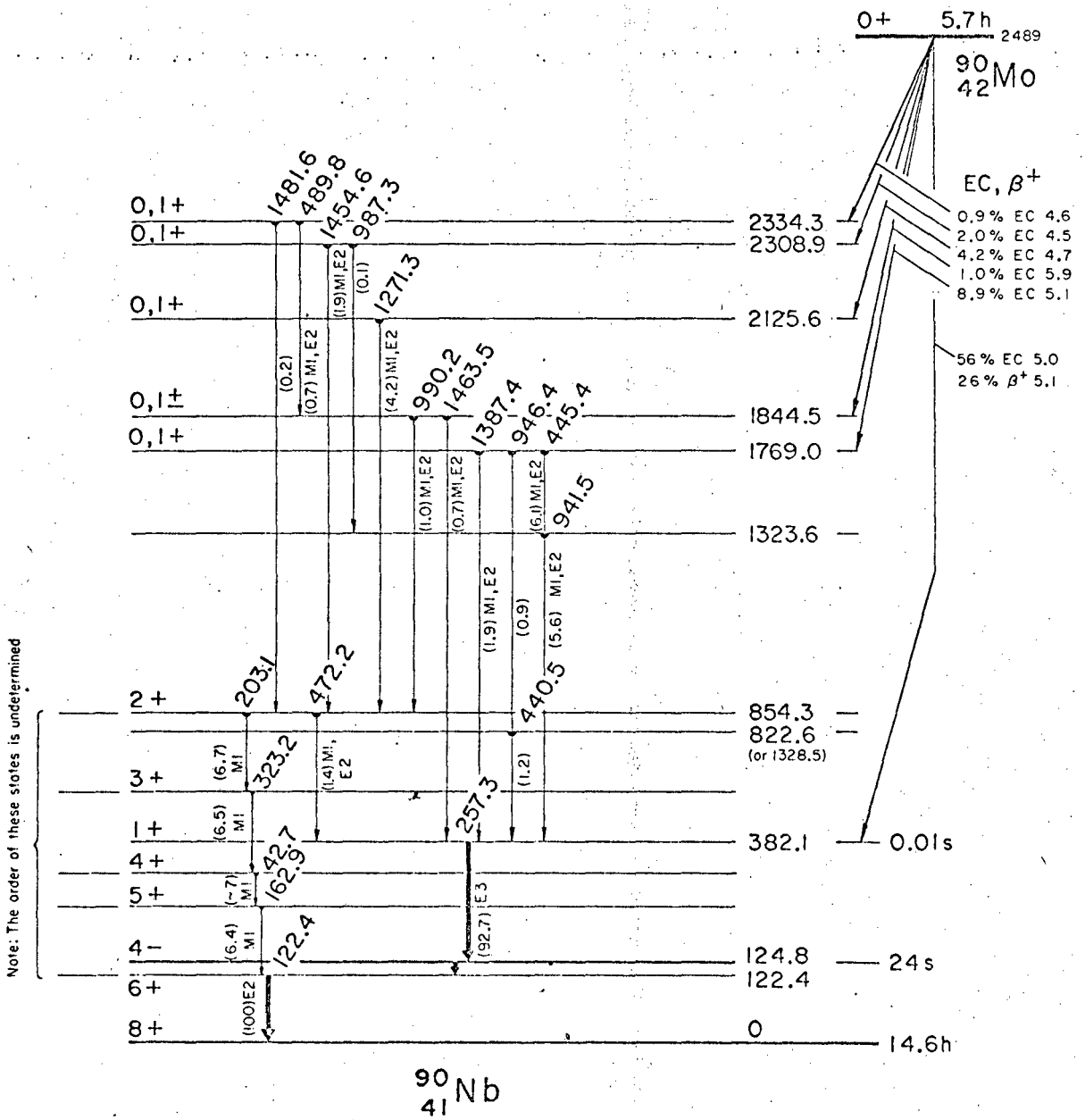

XBL6710-5397

Fig. 4

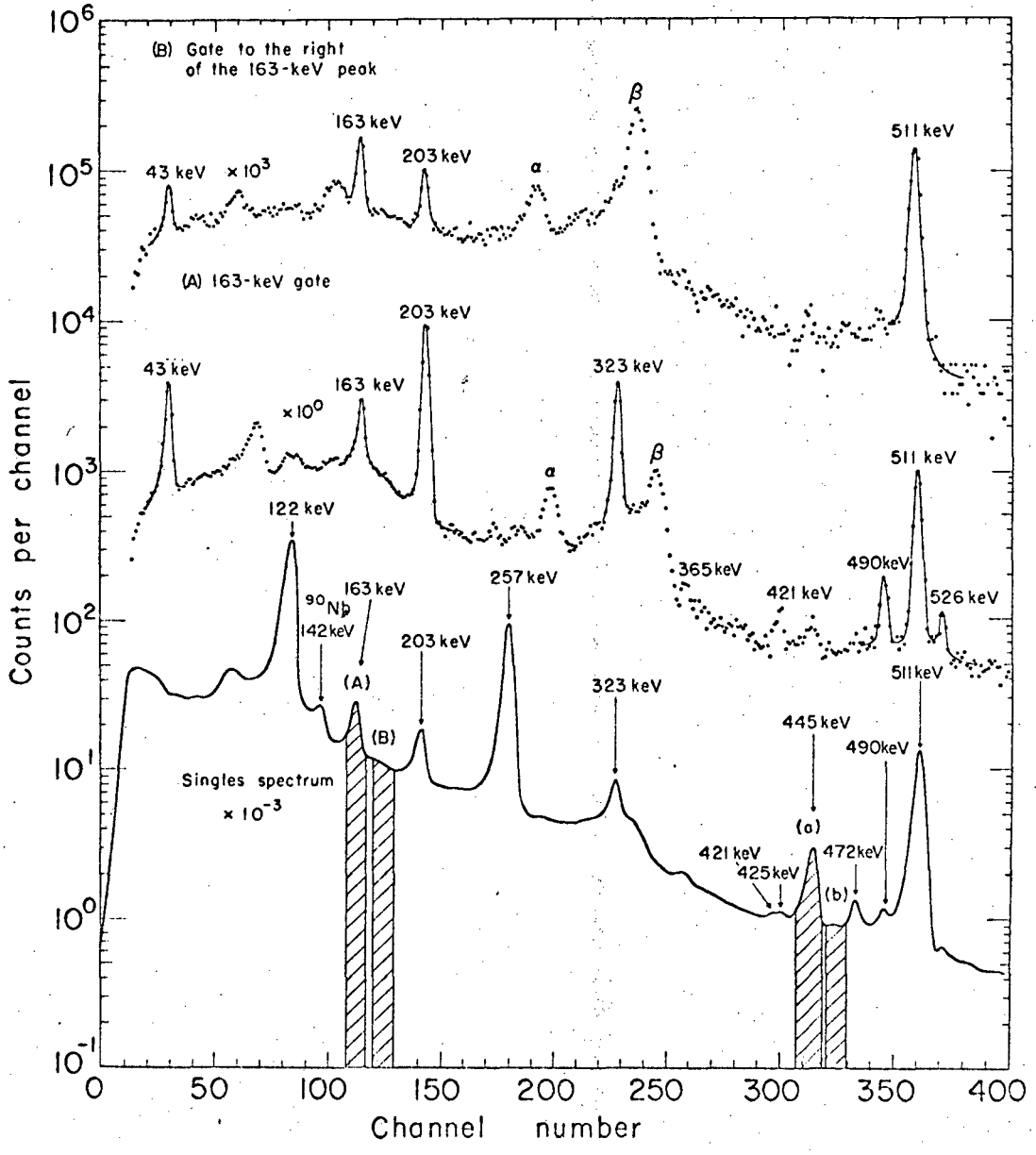

MUB-11978-B

Fig. 5

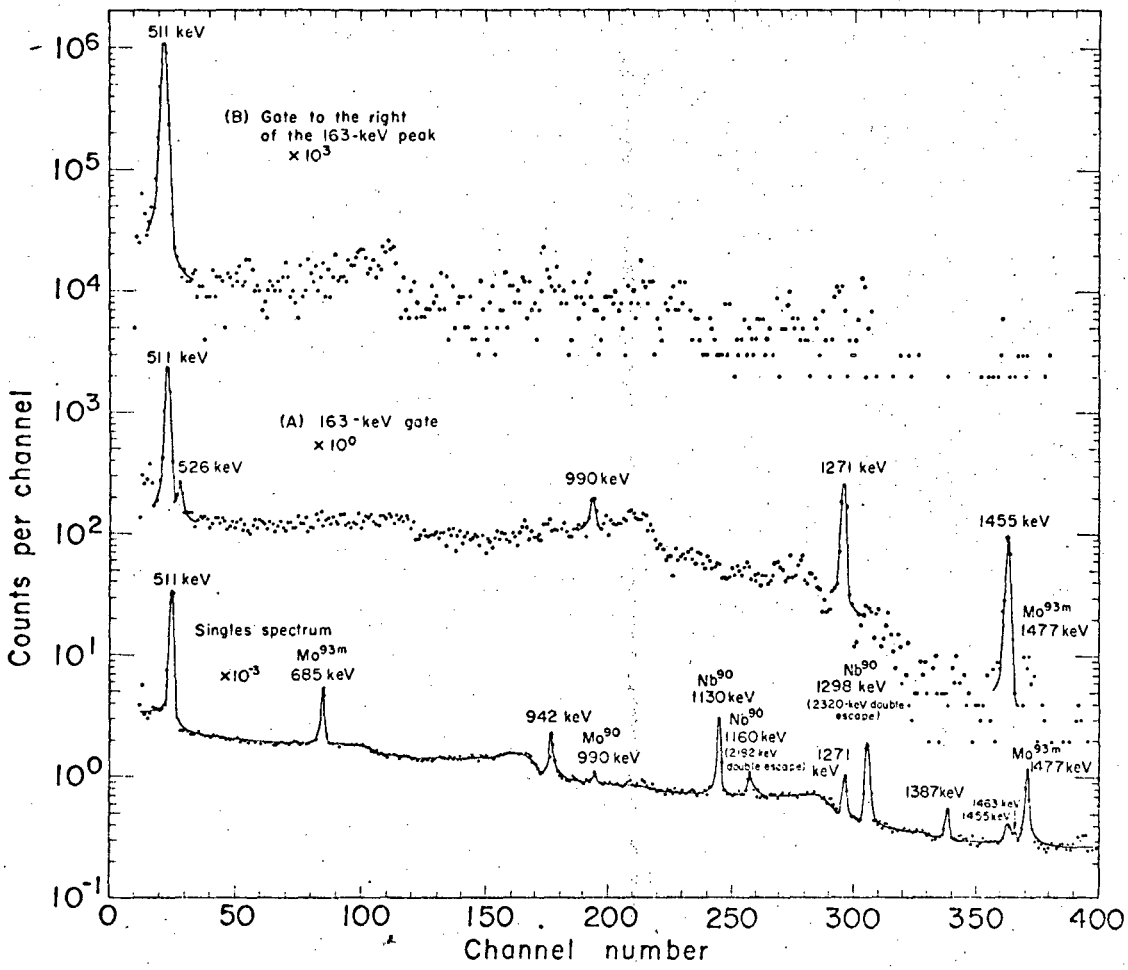

MUB-12571

Fig. 6

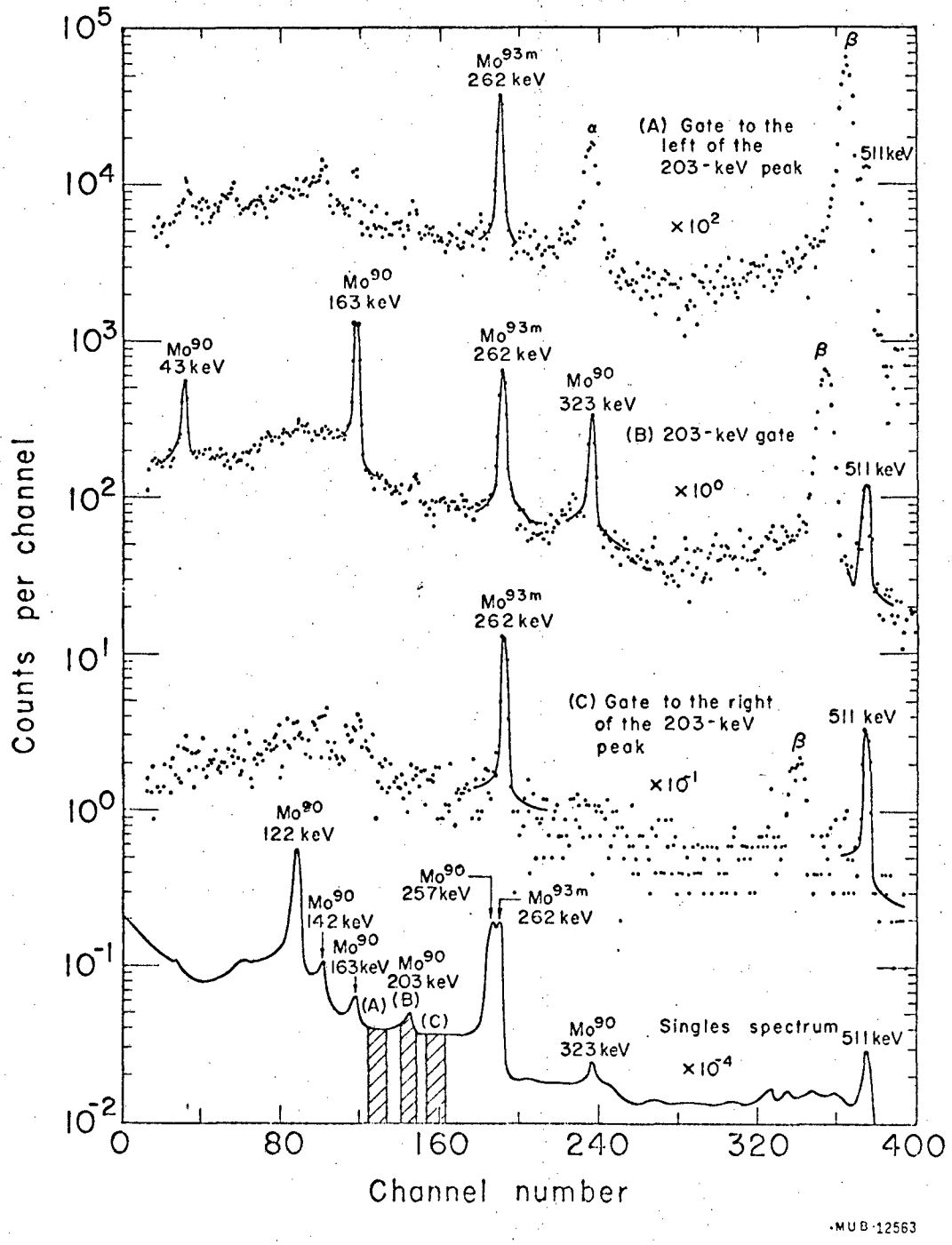
Counts per channel
Channel number
Mo93m 262 keV
(A) Gate to the left of the 203-keV peak
×10²
α
β
511keV
Mo90 163 keV
Mo90 43 keV
Mo93m 262 keV
Mo90 323 keV
(B) 203-keV gate
×10⁰
β
511 keV
Mo93m 262 keV
(C) Gate to the right of the 203-keV peak
×10⁻¹
β
511 keV
Mo90 122 keV
Mo90 142 keV
Mo90 163keV
Mo90 203 keV
(A) (B) (C)
Mo90 257keV
Mo93m 262 keV
Mo90 323 keV
Singles spectrum
×10⁻⁴
511keV
MUB-12563

Fig. 7

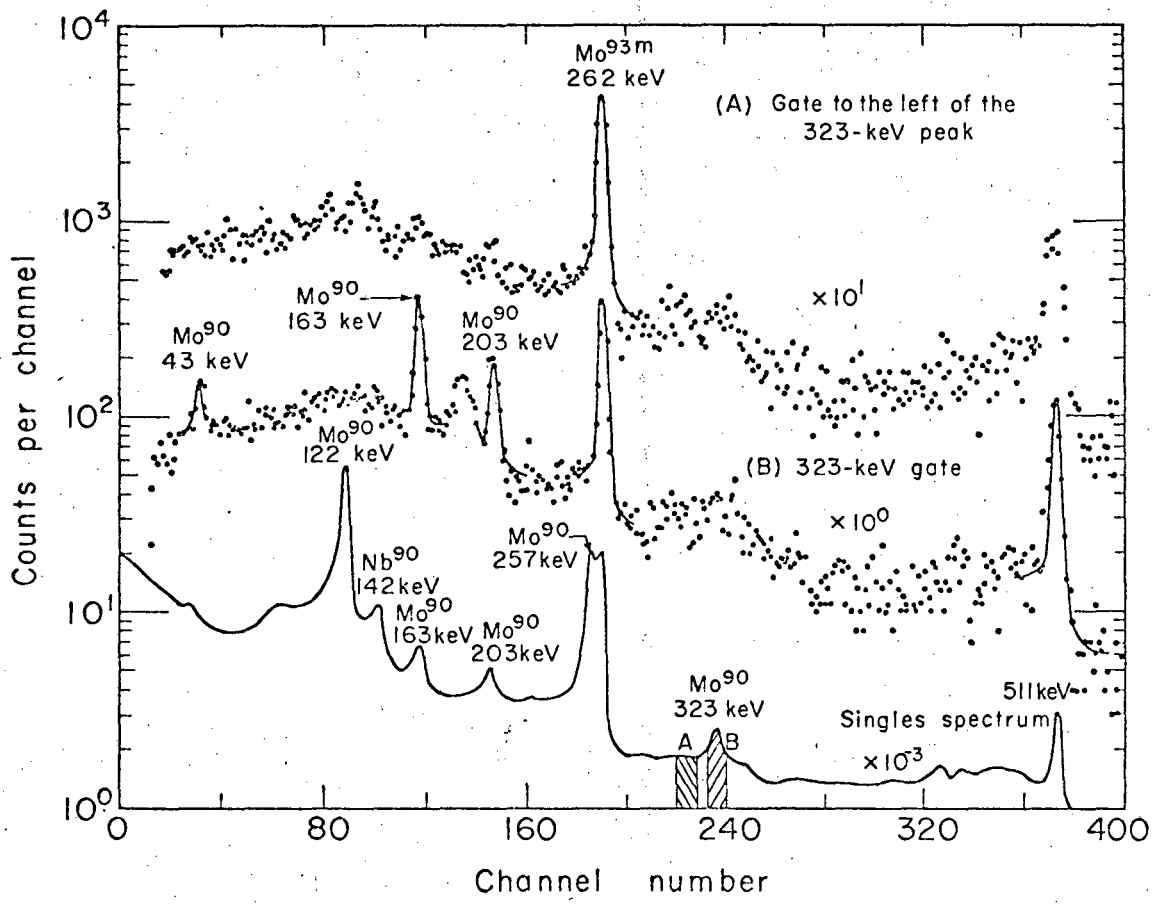
Mo93m
262 keV
(A) Gate to the left of the
323-keV peak
×10¹
Mo90
163 keV
Mo90
203 keV
Mo90
43 keV
Mo90
122 keV
(B) 323-keV gate
×10⁰
Mo90
257keV
Nb90
142keV
Mo90
163keV
Mo90
203keV
Mo90
323 keV
A
B
511keV
Singles spectrum
×10⁻³
Counts per channel
Channel number
10⁴
10³
10²
10¹
10⁰
0
80
160
240
320
400
MUB 11975

Fig. 8

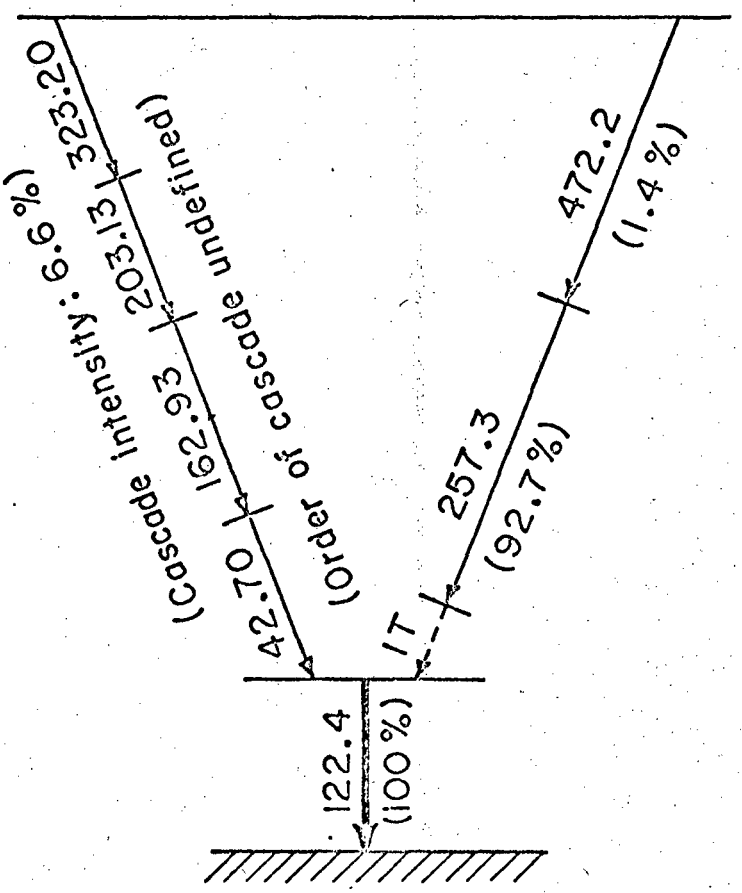

XBL6710-5396

Fig. 9

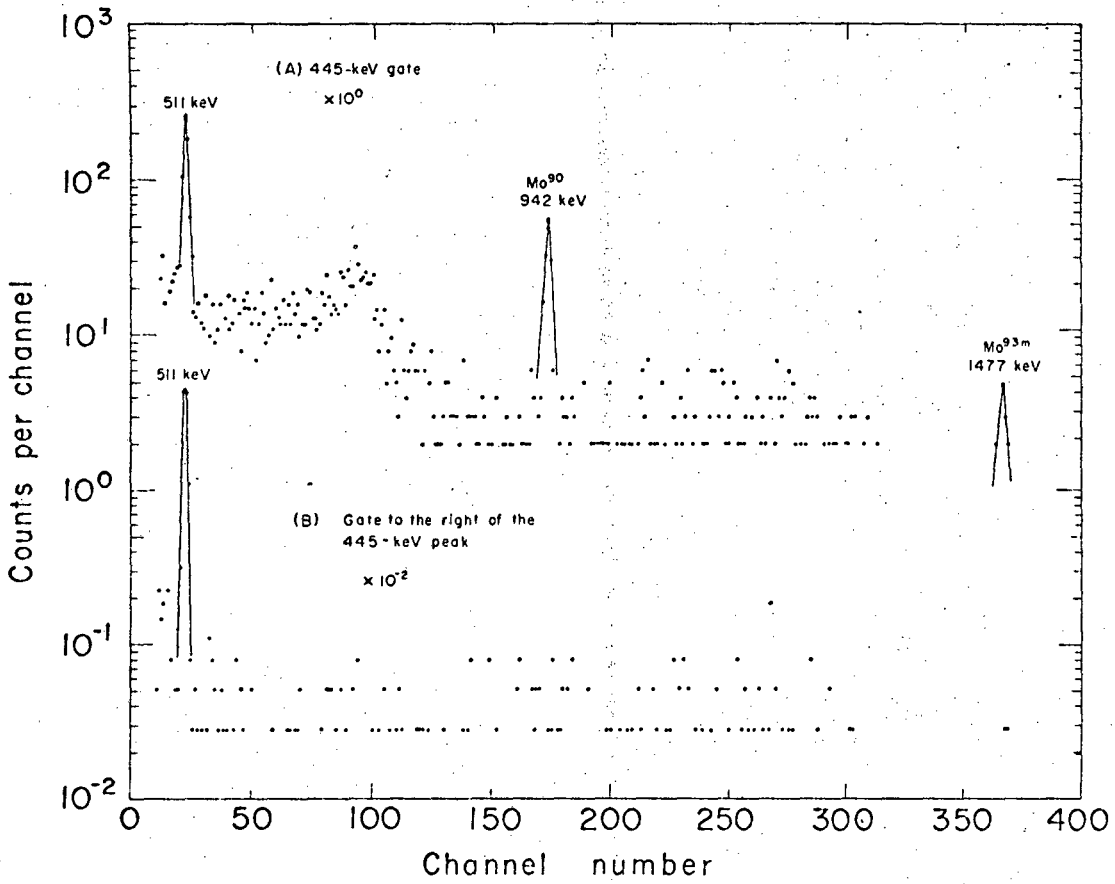

MUB-12573

Fig. 10

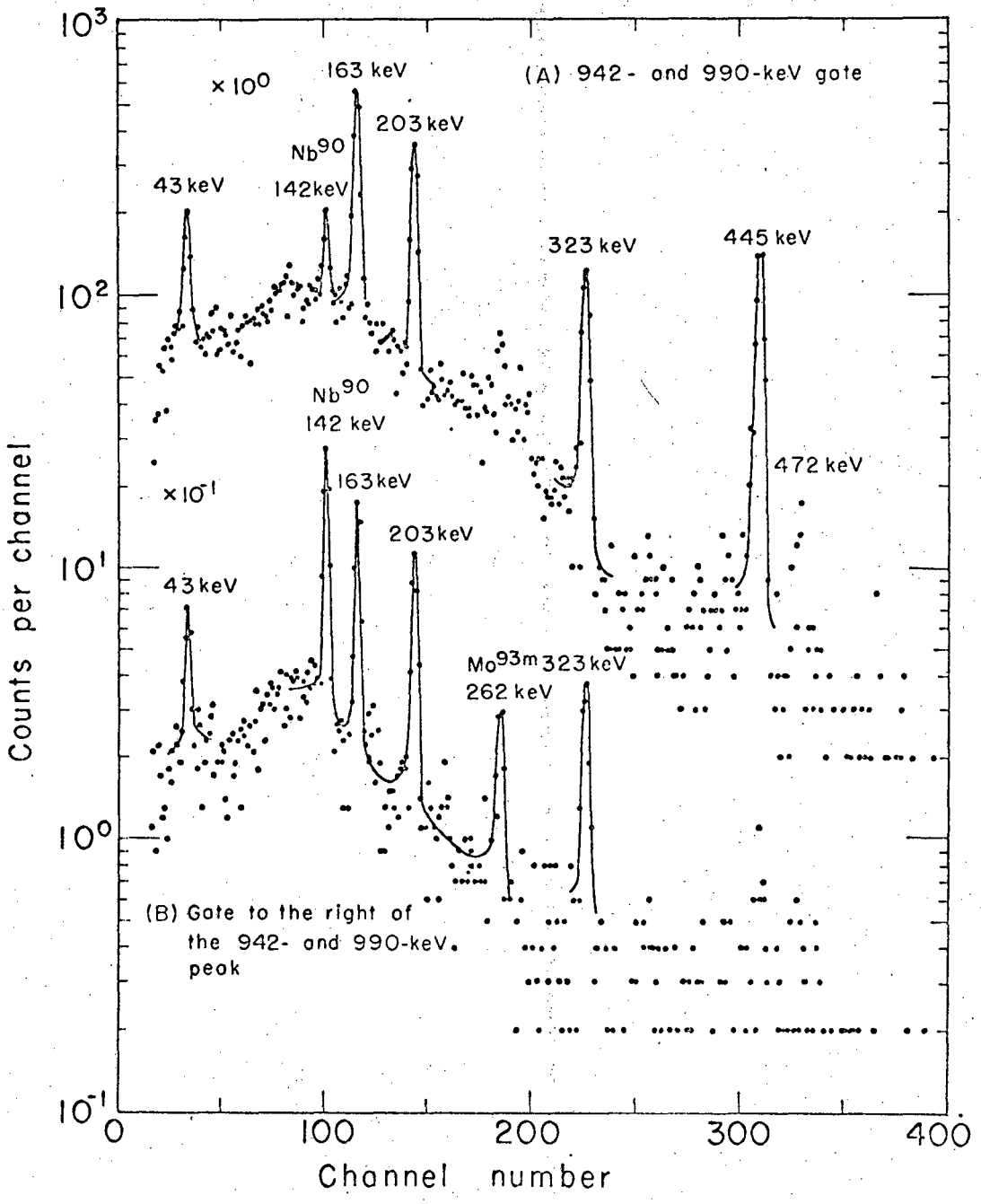
(A) 942- and 990-keV gate
(B) Gate to the right of the 942- and 990-keV peak
Counts per channel
Channel number
43 keV
142 keV
163 keV
203 keV
262 keV
323 keV
445 keV
472 keV
Nb90
Mo93m
×10⁰
×10⁻¹
MUB-11972

Fig. 11

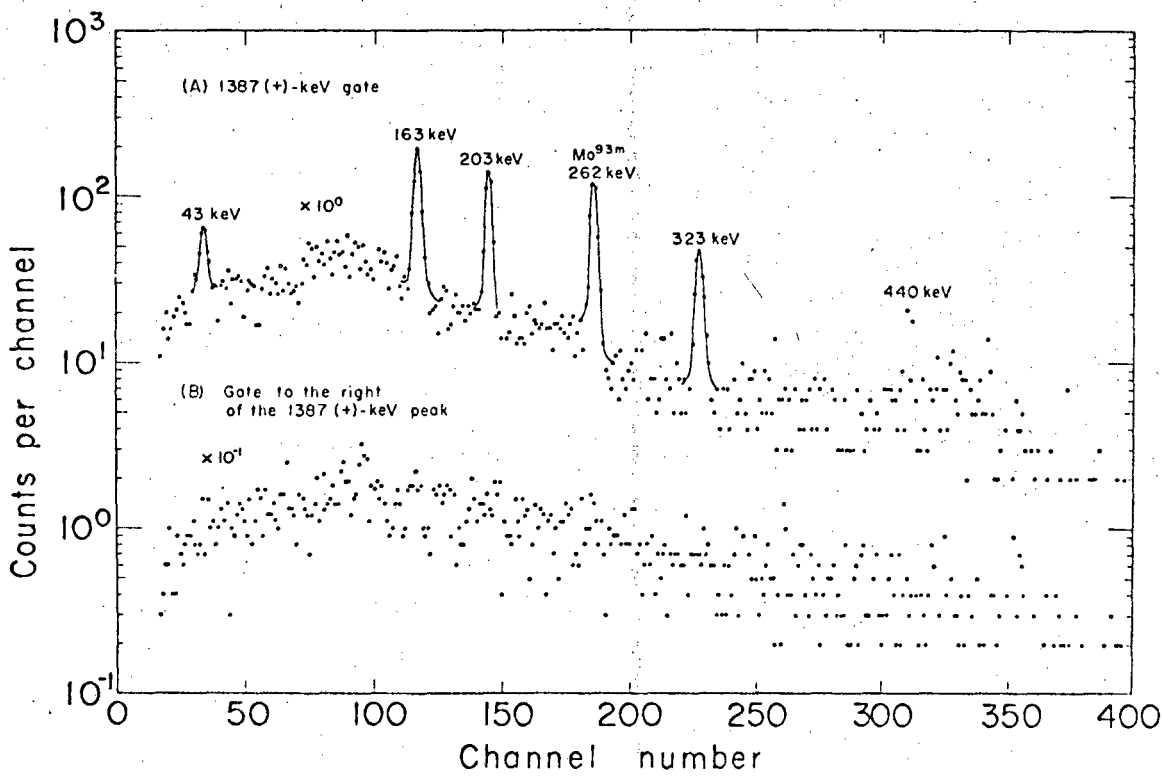

MUB-11977

Fig. 12

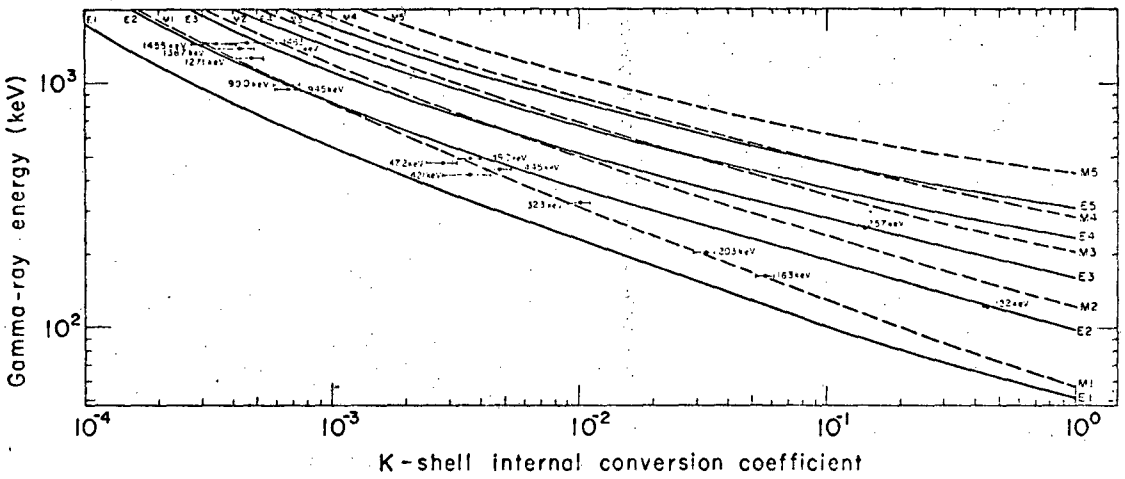

MUB-12578

Fig. 13

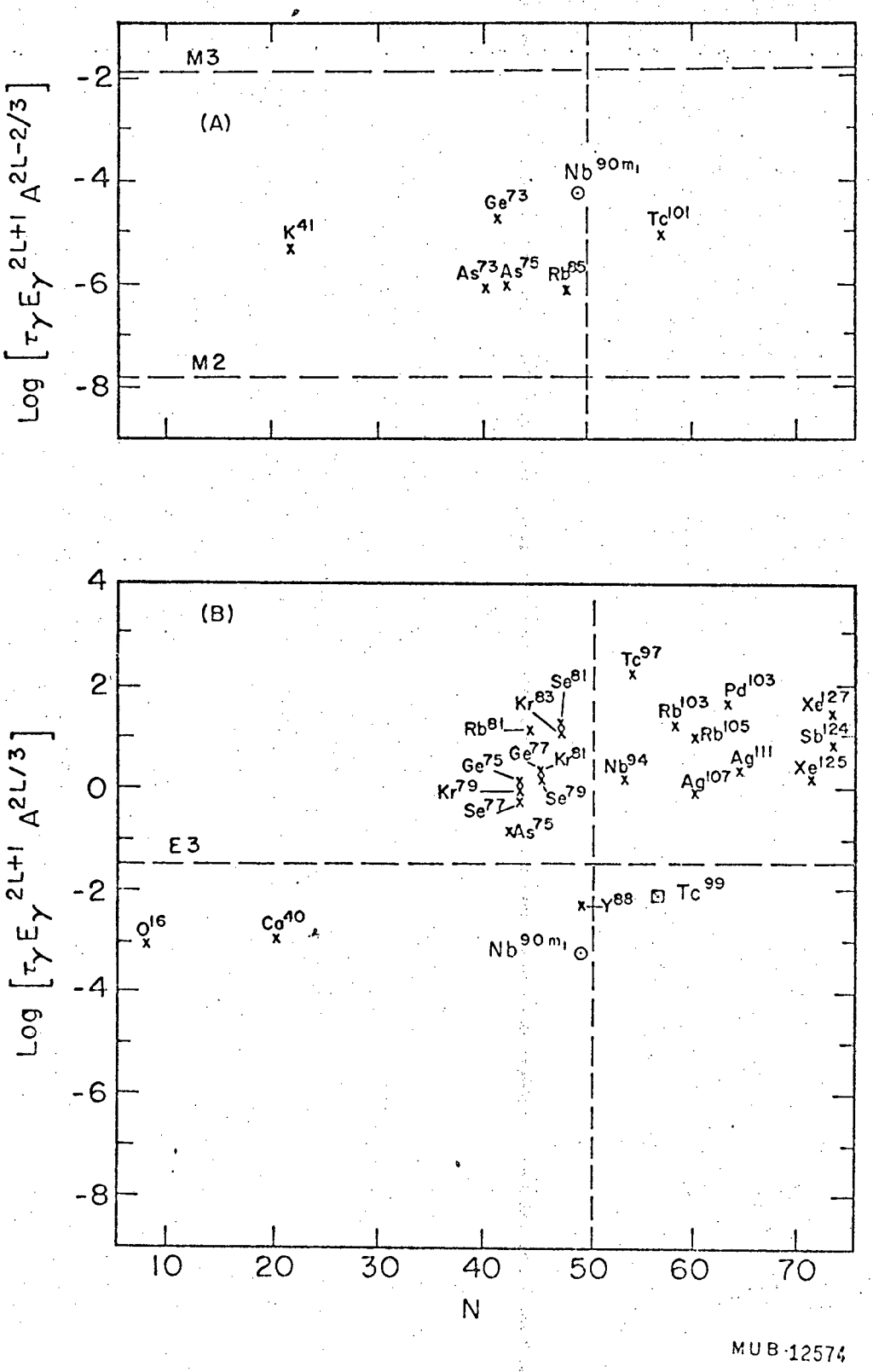
(A)
M3
M2
-2
-4
-6
-8
Log [τγ Eγ 2L+1 A2L-2/3]
Nb 90m1
Ge73
K41
Tc101
As73 As75
Rb85
(B)
E3
4
2
0
-2
-4
-6
-8
Log [τγ Eγ 2L+1 A2L/3]
Tc97
Se81
Kr83
Rb81
Pd103
Rb103
Xe127
xRb105
Sb124
Ge75 Ge77 Kr81
Nb94
Ag111
Ag107
Xe125
Kr79
Se79
Se77
xAs75
Y88
Tc99
O16
Ca40
Nb 90m1
10
20
30
40
50
60
70
N
MUB-12574

Fig. 14

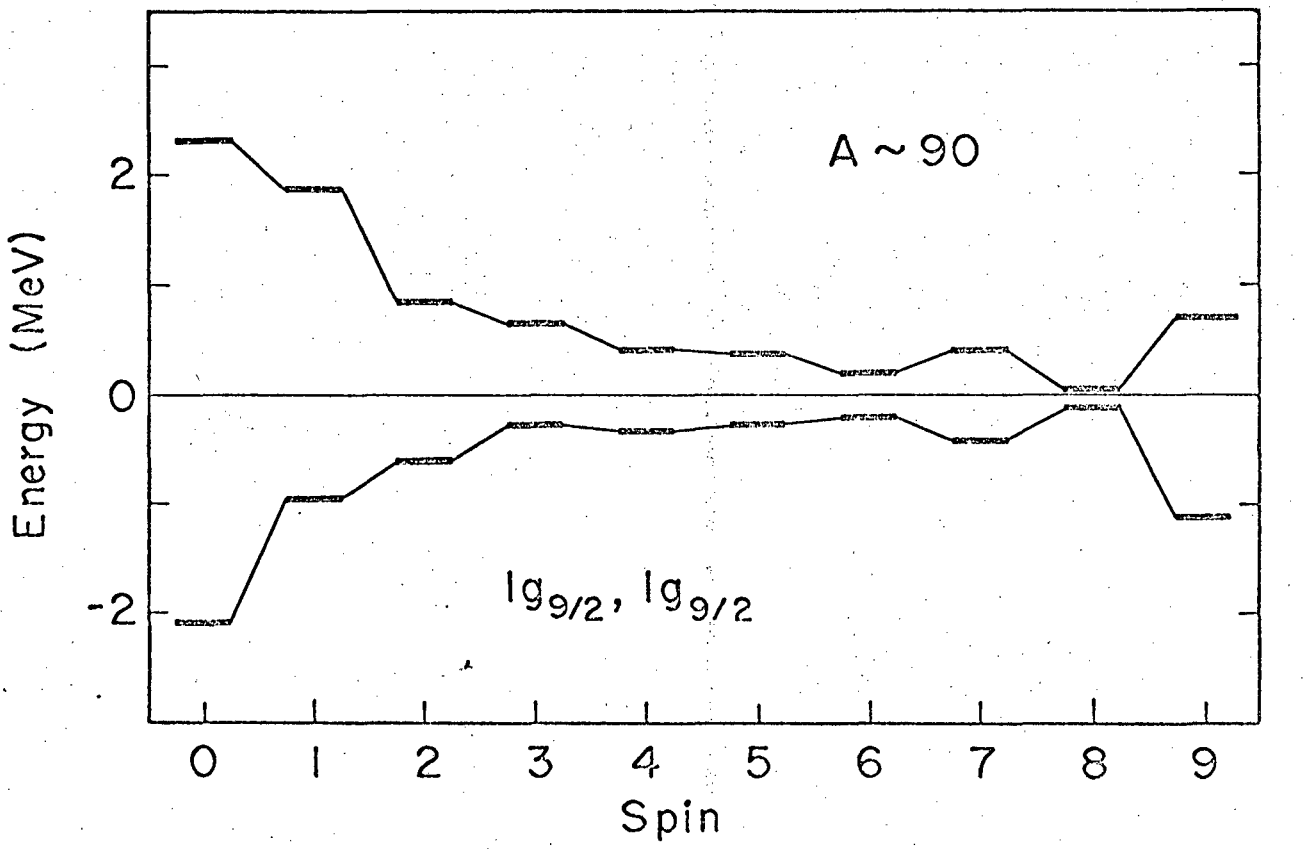

Fig. 15